

A Comparison of Mathematical Models of Left Ventricular Contractility Derived from Aortic Blood Flow Velocity and Acceleration: Application to the Esophageal Doppler Monitor

Glen Atlas, John K.-J. Li and John B. Kostis

Received: 4 April 2014 / Revised: 2 July 2014 / Accepted: 27 July 2014
© The Korean Society of Medical & Biological Engineering and Springer 2014

Abstract

Purpose The esophageal Doppler monitor (EDM) has traditionally been used for minimally-invasive and continuous assessment of both cardiac output and intravascular volume. These measurements are based upon a beat-to-beat analysis of the velocity of distal thoracic aortic blood flow. The purpose of this paper is to compare different mathematical models of LV contractile function which could utilize the EDM and subsequently be determined on a continuous basis. **Methods** This study investigated velocity-based contractility models: peak velocity, (PV); ejection fraction, EF; mean ejection fraction, \overline{EF} ; and maximum LV radial shortening velocity, $\max\left|\frac{dR}{dt}\right|$. Also examined are acceleration-based models: mean acceleration, (MA); force, (F); the maximum rate of rise of systolic arterial blood pressure, $\max\left(\frac{dP}{dt}\right)$; and kinetic energy, (KE).

Results When normalized and subsequently observed on a dimensionless basis, acceleration-based models appear to have a statistically significant greater sensitivity to changes in LV contractility. Furthermore, by combining simultaneous arterial blood pressure measurements with EDM-based flow

information, the components of afterload and their effects on LV contractility could be estimated.

Conclusions Future research is warranted to determine the applicability and limitations of the EDM in continuous assessment of LV contractility and related hemodynamic parameters.

Keywords Esophageal Doppler monitor, Cardiac contractility, Force, Kinetic energy, Heart failure, Modeling

INTRODUCTION

Ejection fraction (EF) is the most commonly used clinical parameter to assess overall left ventricle (LV) contractile performance [1, 2]:

$$EF = \frac{(EDV - ESV)}{EDV}. \quad (1)$$

Where EDV and ESV represent LV end-diastolic volume and end-systolic volume respectively (For this paper, EF is represented as a dimensionless number. However, it is frequently multiplied by 100 and subsequently expressed as a percentage of EDV). It should be noted that EF is frequently utilized by clinicians for the diagnosis, management, and prognostic assessment of those patients with known or suspected systolic or diastolic heart failure (HF) [3] (Systolic and diastolic HF are described within the *Discussion* section).

Stroke volume (SV) is the amount of blood ejected by the LV during systole:

$$SV = (EDV - ESV). \quad (2)$$

Thus, EF is more frequently defined as:

$$EF = \frac{SV}{EDV}. \quad (3)$$

Glen Atlas (✉)
Dept. of Anesthesiology, Professor, Rutgers New Jersey Medical School, Newark, NJ and Dept. of Chemistry, Chemical Biology, and Biomedical Engineering, Adjunct Clinical Professor, Stevens Institute of Technology Hoboken, NJ
Tel : +1-973-758-0758 / Fax : +1-973-758-0405
E-mail : atlasgm@njms.rutgers.edu

John K.-J. Li
Dept. of Biomedical Engineering, Distinguished Professor, Rutgers University, New Brunswick, NJ and College of Biomedical Engineering, Kuang-piu Chair Professor, Zhejiang University, Hangzhou, China

John B. Kostis
Cardiovascular Institute, Associate Dean for Cardiovascular Research, John G. Detwiler Professor of Cardiology, Professor of Medicine & Pharmacology, Rutgers Robert Wood Johnson Medical School, New Brunswick, NJ

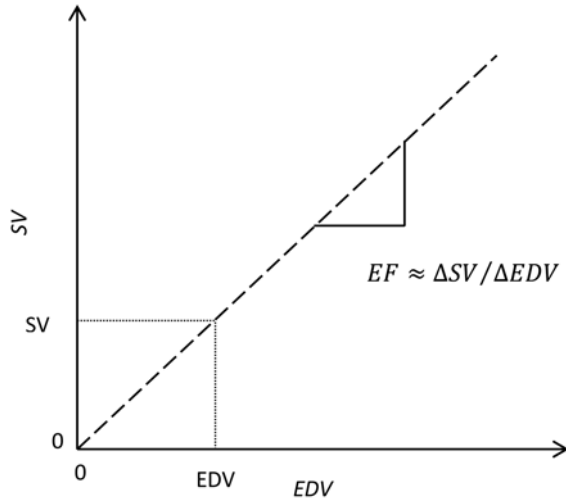


Fig. 1. Under conditions of constant afterload, ejection fraction (EF) can be estimated as the slope of SV vs. EDV. More commonly, EF is calculated as: $EF = SV/EDV$.

The minimally invasive esophageal Doppler monitor (EDM) provides both an excellent approximation and trend analysis of SV [4, 5]. This is attained on a continuous or “beat-to-beat” basis.

Note that EF remains relatively constant in spite of changes in volume status [6]. However, EF can be affected by changes in afterload [7]. Clinically, pharmacologic agents which reduce afterload and/or preload are frequently utilized in the management of those patients with documented or suspected HF [8].

In addition, EF can be considered as the approximate slope of the SV vs. EDV relationship [6]. Consequently, with a constant afterload, EF may also be estimated as: $EF \approx \Delta SV/\Delta EDV$. This is illustrated in Fig. 1. Pharmacologic reductions in afterload would therefore be associated with increases in the slope of this line.

It should be noted that stroke distance (SD) can be calculated using the definite integral of the velocity of distal thoracic aortic blood flow, $v(t)$ [9]:

$$SD = k \cdot \int_0^{FT} v(t) dt = k \cdot SD_a \tag{4}$$

Where SD_a represents the distance that blood flows, during systole, within the distal thoracic aorta. Note that a dimensionless multiplicative factor ($k = 1.4$) is used to augment or “correct” SD_a for that portion of cardiac output (CO) which does not “reach” the distal thoracic aorta and is thus not directly measured by the EDM. This includes blood flow to the carotid, vertebral, and subclavian arteries [10]. Other means of correlating distal thoracic aortic blood flow, with total CO, have also been described [10, 11].

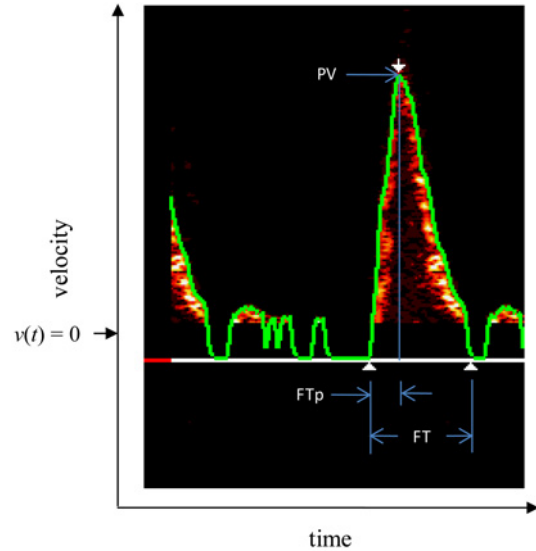


Fig. 2. The esophageal Doppler monitor (EDM) displays the velocity of distal thoracic aortic blood flow as a function of time. Peak velocity (PV), flow time to peak velocity (FTp), and flow time (FT) are illustrated. Note the location of zero velocity on the ordinate.

Moreover, systolic ejection time is referred to as flow time (FT) (The systolic ejection time, or FT, is also known as left ventricle ejection time (LVET)). This is the time period from the opening of the aortic valve until its closing. Fig. 2 depicts the velocity of distal thoracic aortic blood flow, measured by an EDM, during clinical use.

In evaluating LV contractility, EF is typically used. Whereas the maximum rate of rise of systolic blood pressure, $\max(\frac{dP}{dt})$, has been occasionally utilized in the clinical setting [12]. There have also been attempts of using peak blood flow velocity and acceleration for assessing LV contractility [12].

In this paper, we will compare different mathematical models of LV contractile function which could utilize the EDM. These include velocity-based models: peak velocity, (PV); EF; mean ejection fraction, \overline{EF} ; and maximum LV radial shortening velocity, $\max|\frac{dR}{dt}|$. Also examined are acceleration-based models: mean acceleration, (MA); force, (F); the maximum rate of rise of systolic arterial blood pressure, $\max(\frac{dP}{dt})$; and kinetic energy, (KE). Moreover, this paper demonstrates that acceleration-based models appear to have a greater sensitivity to changes in LV contractility than those which are velocity-based.

METHODS AND ANALYSIS

As shown in Fig. 3, SV can be represented as a cylinder; with a volume associated with the opening ($t = 0$) and closing ($t = FT$) of the aortic valve:

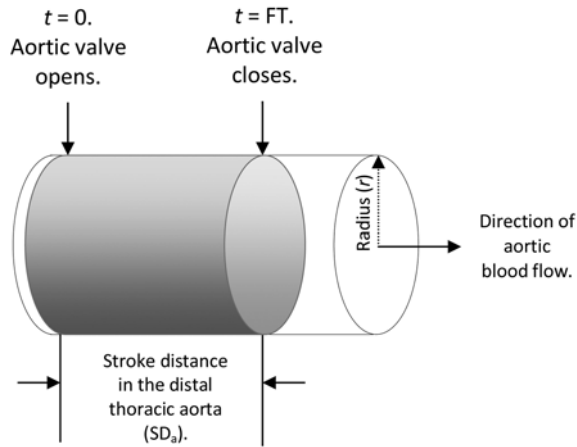


Fig. 3. Stroke volume (SV) can be modeled as a cylinder; with a length proportional to stroke distance in the distal thoracic aorta (SD_a) and a cross-sectional area based upon aortic radius (r). This relationship is described using Eqs. (4-6).

$$SV = A \cdot SD. \tag{5}$$

Where A represents aortic cross-sectional area:

$$A = \pi \cdot r^2. \tag{6}$$

Aortic radius is defined as a time-invariant constant, r . By substitution, EF is then:

$$EF = \frac{A \cdot SD}{EDV} = \frac{\pi \cdot r^2 \cdot SD}{EDV}. \tag{7}$$

Clinically, r can be reliably estimated based upon each individual patient’s age, gender, height, and weight [13].

The use of concomitant ultrasonic M-mode has also been utilized to directly measure distal thoracic aortic diameter in real time. This feature also allows for optimum and time-efficient focusing of the EDM probe onto the aorta [10]. However, current EDMs are either not manufactured with this feature or do not fully utilize it (Deltex Medical (UK) does not employ M-mode ultrasound in their EDM. Whereas Atyx Medical (France) incorporates this feature only to facilitate probe focusing; rather than aortic diameter measurement).

By combining (4) and (7), the following expression results:

$$EF = \frac{k \cdot \pi \cdot r^2}{EDV} \cdot \int_0^{FT} v(t) dt. \tag{8}$$

It should be noted that mean or average velocity, \bar{v} , is defined as:

$$\bar{v} = \frac{1}{FT} \cdot \int_0^{FT} v(t) dt. \tag{9}$$

Utilizing (4) and (9), SD can then be expressed as a function of *both* \bar{v} and FT:

$$SD = k \cdot \bar{v} \cdot FT. \tag{10}$$

Substitution then yields:

$$EF = \frac{k \cdot \pi \cdot r^2 \cdot \bar{v} \cdot FT}{EDV}. \tag{11}$$

Thus, EF can be represented as a function which incorporates r , \bar{v} , and FT. Additionally, changes in EF would be directly proportional to changes in \bar{v} . Recent clinical EDM research supports this [14].

The physiological importance, of EF as expressed using (11), is clinically very significant. Specifically, vasodilation or reductions in afterload can result in increases in either r , \bar{v} , or FT which are associated with increases in EF [14-16]. However, it should be noted that the relatively small change in aortic diameter, occurring between diastole and systole, does not alter the clinical utility of the EDM. Thus, the assumption of a “fixed” aortic diameter has demonstrated that the EDM provides a useful approximation of both SV and subsequent CO [4, 5]. In addition, this information can be provided to the clinician on a near-instantaneous basis.

Furthermore, although the EDM cannot measure EDV, both the velocity and acceleration of proximal aortic blood flow have been shown to correlate with EF [17, 18]. If EF is foreknown (This can be done at the patient’s bedside or as part of a preoperative cardiac work-up) and afterload remains relatively constant, approximate clinical evaluations of EDV could then be made with an EDM: $EDV = \frac{SV}{EF}$.

It should be noted that the EDM measures aortic blood flow only slightly “downstream” from the aortic root (This is approximately at the level of the T6 dermatome). Using the EDM, MA of distal thoracic aortic blood flow is accurately estimated as:

$$MA = \frac{PV}{FTp}. \tag{12}$$

Note that this closely approximates true average acceleration; as $v(t)$ increases from zero at $t = 0$ to PV at $t = FTp$.

Other imaging modalities, such as transesophageal or transthoracic echocardiography, can be used to assess both EDV and the velocity of aortic blood flow. However, these techniques may be difficult to use on a continuous basis; in either an operating room or intensive care setting. Whereas the EDM probe can remain within a patient for up to 10 days due to the probe’s small diameter and flexibility. Furthermore, awake nasal placement of the EDM probe has been successfully reported [19, 20].

The EDM can also be readily utilized in patients who are in non-supine positions [21, 22]. As the EDM’s determination

of the velocity of distal thoracic aortic blood flow is pressure-independent, its measurements may consequently be position-independent. Thus, the EDM may not be affected by changes in hydrostatic pressure which would accompany changes in patient position. Further research to elucidate the EDM's role in "non-supine" patient monitoring is therefore necessary. Nonetheless, the EDM appears to consistently produce excellent "trend" data when utilized with patients who are in non-supine positions (Unpublished clinical observations by the first author (GA). Note that both supine and non-supine patient positioning is frequently utilized during surgical procedures requiring hemodynamic monitoring. However, the angle of the EDM probe, relative to the aorta, may subsequently change as patients are moved from supine to non-supine positions).

Moreover, EF can be represented as a function of time, $EF(t)$. This is accomplished by initially describing SD as a function of time, $SD(t)$, using the indefinite integral of $v(t)$:

$$SD(t) = k \cdot \int v(t)dt + C \quad 0 \leq t \leq FT. \tag{13}$$

Thus:

$$EF(t) = \frac{k \cdot \pi \cdot r^2}{EDV} \cdot \{ \int v(t)dt + C \} \quad 0 \leq t \leq FT. \tag{14}$$

By combining (13) and (14) (The constant of integration, C , is chosen so that $SD(0) = EF(0) = 0$):

$$EF(t) = \frac{\pi \cdot r^2}{EDV} \cdot SD(t) \quad 0 \leq t \leq FT. \tag{15}$$

It should be noted that $SD(t)$ is evaluated throughout the entire time-course of systolic ejection. Furthermore, $SD(t)$ could be assessed in real time by an EDM; with minimal modification to its existing software.

Note that $EF(t)$ and $SD(t)$ are directly proportional. Furthermore, the boundary conditions of (15) are such that: $EF(0) = 0$ and $EF(FT) = EF$. The sigmoid characteristics of $EF(t)$ are illustrated and discussed in "Numerical Examples" (Note that $SD(t)$ is not available in current commercially-manufactured EDMs).

Additionally, the first and second derivatives of $EF(t)$ can be examined. These illustrate how velocity, $v(t)$, and acceleration, $a(t)$, are associated with $EF(t)$:

$$\frac{d[EF(t)]}{dt} = \frac{k \cdot \pi \cdot r^2}{EDV} \cdot v(t) \quad 0 \leq t \leq FT. \tag{16}$$

Similarly, since $a(t) = \frac{dv}{dt}$:

$$\frac{d^2[EF(t)]}{dt^2} = \frac{k \cdot \pi \cdot r^2}{EDV} \cdot a(t) \quad 0 \leq t \leq FT. \tag{17}$$

\overline{EF} is defined as the time-averaged value of $EF(t)$ during systolic ejection. This parameter may be potentially useful during real-time clinical contractility assessment:

$$\overline{EF} = \frac{1}{FT} \cdot \int_0^{FT} EF(t)dt. \tag{18}$$

Application of the modified logistic equation

The modified logistic equation is an empirical model of the velocity of aortic blood flow [9]:

$$v(t) = \alpha \beta e^{-\gamma t} \left(1 - \frac{t}{FT} \right) \quad 0 \leq t \leq FT. \tag{19}$$

Where α has units of acceleration and β is dimensionless. For simplicity, α and β can be combined as a product and subsequently expressed as a single term. It should also be noted that the LV is modeled as a time-dependent amplifier with an exponentially-decaying gain. Fig. 4 illustrates this. In addition, both the right and left ventricles, in terms of blood flow velocity, are represented.

Fig. 2 is a graph of the velocity of distal thoracic aortic blood flow vs. time. Note that (19) is utilized for the EDM-based hemodynamic modeling of this velocity vs. time relationship. Eq. (19) will be further explored in "Numerical Examples."

The exponentially-decaying time-dependent amplifier employs a term, γ , which is expressed using the dimension of inverse time [9]:

$$\gamma = \frac{2 - \left(\frac{FT}{FTp} \right)}{(FTp - FT)} \quad 0 < FTp < FT. \tag{20}$$

Furthermore, FT and FTp are illustrated in Fig. 2.

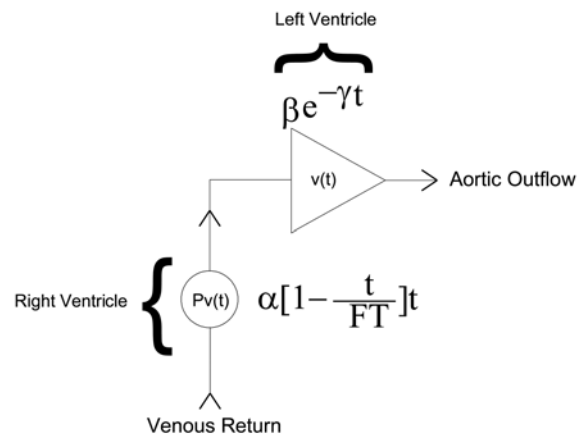


Fig. 4. The velocity of blood flow from the left ventricle, $v(t)$, is illustrated as a time-dependent amplifier with an exponentially decaying gain. Whereas the velocity of blood flow from the right ventricle is represented as $Pv(t)$ [9].

By substituting (19) into (4), the resulting indefinite integral, $SD_a(t)$, is subsequently determined [9] (*Appendix A* documents $v(t)$, as well as its first derivative and indefinite integral, using a difference of two Taylor’s series):

$$\int v(t)dt + C = SD_a(t) = \left[\left(\frac{t}{FT} - 1 \right) t + \left(2 \frac{t}{FT} - 1 \right) \frac{1}{\gamma} + \frac{2}{FT\gamma^2} \right] \frac{\alpha\beta}{\gamma} e^{-\gamma t} - \left(-1 + \frac{2}{FT\gamma} \right) \frac{\alpha\beta}{\gamma^2} \quad 0 \leq t \leq FT. \tag{21}$$

Eq. (21) can also be represented as a definite integral which is evaluated over the time-course of FT.

The sphere-to-cylinder model

Furthermore, $EF(t)$ can also be modeled using two components: a *contracting sphere*, representing the LV, ejecting into a rigid *cylinder* representing the aorta. This is illustrated in Fig. 5. The use of this model produces a straightforward approximate representation of the interaction between the LV and the aorta. It also allows for a comprehensive comparison of the different means of assessing the relationship between LV contraction and the subsequent flow of blood through the aorta. Additionally, the “sphere-to-cylinder” model clearly and succinctly demonstrates the potential utility of the EDM in assessing continuous LV contractility. Although the LV is more hemiellipsoid than spherical in its structure, this representation nonetheless produces similar results when compared with preliminary clinical observations [23].

The equivalent spherical radius associated with LV EDV would therefore be:

$$R_{EDV} = \sqrt[3]{\frac{3}{4\pi} EDV} = \sqrt[3]{\frac{3}{4\pi} \left(\frac{SV}{EF} \right)}. \tag{22}$$

In a similar manner, the spherical radius associated with LV ESV would be represented as:

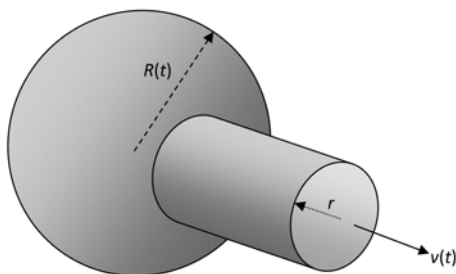


Fig. 5. A sphere-to-cylinder model can be used to represent the contraction of the LV and the subsequent flow of blood into the aorta. Note that the sphere has a time-dependent radius, $R(t)$. Whereas the radius of the aorta, r , is assumed constant. The velocity of the aortic blood flow is represented as $v(t)$.

$$R_{ESV} = \sqrt[3]{\frac{3}{4\pi} ESV} = \sqrt[3]{\frac{3}{4\pi} (EDV - SV)}. \tag{23}$$

The contracting sphere would subsequently have a time-varying radius, $R(t)$, with the following boundary values: $R(0) = R_{EDV}$ and $R(FT) = R_{ESV}$. Using this model and (15), $EF(t)$ would then be:

$$EF(t) = \frac{\pi \cdot r^2}{EDV} \cdot SD(t) = \frac{EDV - \frac{4}{3}\pi R^3(t)}{EDV} = \frac{R_{EDV}^3 - R^3(t)}{R_{EDV}^3} \quad 0 \leq t \leq FT. \tag{24}$$

After rearranging (22), further substitution then yields:

$$EF(t) = \frac{\pi \cdot r^2}{\frac{4}{3}\pi R_{EDV}^3} \cdot SD(t) = \frac{R_{EDV}^3 - R^3(t)}{R_{EDV}^3} \quad 0 \leq t \leq FT. \tag{25}$$

It is clear that at beginning systole or end-diastole, $R(0) = R_{EDV}$. Note that the above equations apply during FT only.

Simplifying and solving for $R(t)$:

$$R(t) = \sqrt[3]{\left(R_{EDV}^3 - \frac{3}{4}r^2 SD(t) \right)} \quad 0 \leq t \leq FT. \tag{26}$$

Eq. (26) is clinically significant in that it models the time-varying radius of the LV as a function of SD; as measured by an EDM.

Note that (26) can also be derived using the continuity principle. Where flow, $Q_c(t)$, in the cylinder is equated to that generated by the contracting sphere, $Q_s(t)$:

$$Q_s(t) = Q_c(t) \quad 0 \leq t \leq FT. \tag{27}$$

Initially, the volume of blood ejected from the sphere as a function of time, $V(t)$, is defined as:

$$V(t) = \frac{4}{3}\pi (R_{EDV}^3 - R^3(t)) \quad 0 \leq t \leq FT. \tag{28}$$

The flow rate from the contracting sphere is then:

$$Q_s(t) = \frac{dV}{dt} = -4\pi R^2(t) \frac{dR}{dt} \quad 0 \leq t \leq FT. \tag{29}$$

Note that $\frac{dR}{dt} \leq 0$ and $Q_s(t) \geq 0$ throughout systolic ejection. Whereas the flow in the cylinder, with its fixed radius of r , is:

$$Q_c(t) = k\pi r^2 \cdot v(t) \quad 0 \leq t \leq FT. \tag{30}$$

Equating (29) and (30) yields:

$$-4\pi R^2(t) \frac{dR}{dt} = k\pi r^2 \cdot v(t) \quad 0 \leq t \leq FT. \tag{31}$$

Simplifying:

$$-4 \frac{R^2(t) dR}{r^2 dt} = k \cdot v(t) \quad 0 \leq t \leq FT. \tag{32}$$

Eq. (32) is physiologically important in that it explains how small increases, in the radius of the contracting LV, would produce significant increases in the velocity of blood flow in the aorta. Clinically, this could be applied in both the quantitative interpretation of observed flow rate changes and the utilization of the Frank-Starling mechanism.

Thus, the effect of volume loading, resulting in a “fuller” or “better-filled” ventricle, would maximize the velocity of the ejected aortic blood flow [23]. Note that this applies to an LV which has normal contractility rather than one which is “failing” secondarily to volume overload.

Furthermore, (32) also demonstrates that $v(t)$ is not directly proportional to $\frac{dR}{dt}$. In fact, this relationship has been modeled as a nonlinear nonhomogeneous first order differential equation with a variable coefficient.

By multiplying both the left and right hand sides of (32) by differential time, dt , a subsequent *indefinite* integral relationship can be expressed (Appendix B demonstrates the derivation of SV using this equation represented as a definite integral):

$$\frac{-4}{r^2} \int R^2(t) dR = k \cdot \int v(t) dt + C_R \quad 0 \leq t \leq FT. \tag{33}$$

The solution of (32) is thus based upon a separation of variables technique, as demonstrated in (33), and is:

$$R^3(t) = R_{EDV}^3 - \frac{3}{4} r^2 SD(t) \quad 0 \leq t \leq FT. \tag{34}$$

Knowing that $SD(0) = 0$, the constant of integration, C_R , is subsequently chosen so that: $R(0) = R_{EDV}$. Thus, the application of the continuity principle yields the same result for $R(t)$ as (26):

$$R(t) = \sqrt[3]{\left(R_{EDV}^3 - \frac{3}{4} r^2 SD(t)\right)} \quad 0 \leq t \leq FT. \tag{35}$$

Substituting (22) into either (35) or (26):

$$R(t) = \sqrt[3]{\left(\frac{3 \cdot SV}{4\pi(EF)} - \frac{3}{4} r^2 SD(t)\right)} = \left(\frac{3}{4}\right)^{\frac{1}{3}} \cdot \sqrt[3]{\frac{SV}{\pi(EF)} - r^2 SD(t)} \quad 0 \leq t \leq FT. \tag{36}$$

Clinically, (36) is potentially useful; as $R(t)$ is difficult to measure under routine clinical conditions. Furthermore, the EDM intrinsically calculates and subsequently displays SV. In addition, EF is frequently determined preoperatively using transthoracic echocardiography. Thus, once $R(t)$ is established, $\frac{dR}{dt}$ could then be numerically calculated using a finite-difference technique (Eq. (41) illustrates another method for determining $\frac{dR}{dt}$).

Within the aorta, the time to peak flow (FTp) occurs *prior* to the time of the peak of the absolute value of $\frac{dR}{dt}$ within the LV [24, 25]. This can be examined when the acceleration of aortic blood flow is zero. By differentiating (32) and subsequently equating $\frac{dv}{dt}$ to zero:

$$\frac{-4R(t)}{r^2} \left[R(t) \frac{d^2R}{dt^2} + 2 \cdot \left(\frac{dR}{dt}\right)^2 \right] = 0. \tag{37}$$

Inspection of (37) reveals that $\frac{d^2R}{dt^2}$ must be less than zero for $\frac{dv}{dt}$ to equal zero. Thus, FTp must occur on the corresponding “falling slope” side of $\frac{dR}{dt}$.

Similarly, $\frac{dR}{dt}$ has its maximum absolute value occurring on the corresponding “falling slope” side of $\frac{dv}{dt}$. Differentiating (32) yields:

$$\frac{-4R(t)}{r^2} \left[R(t) \frac{d^2R}{dt^2} + 2 \cdot \left(\frac{dR}{dt}\right)^2 \right] = k \frac{dv}{dt}. \tag{38}$$

Inspection of (38) reveals that when $\frac{d^2R}{dt^2} = 0$, $\frac{dv}{dt}$ must be less than zero. Thus it cannot be assumed that peak flow, within the aorta, occurs simultaneously with peak $\frac{dR}{dt}$ of the LV wall. This relationship is illustrated in Fig. 6. This further illustrates that the velocity of aortic blood flow has both a considerably different magnitude and time-course than that of LV radial shortening velocity.

Clinical examinations of LV radial shortening velocity have demonstrated numerically similar results, in humans, as that predicted by the sphere-to-cylinder model [24, 26]. Furthermore; the sphere-to-cylinder model allows for a both a concise and comprehensive comparison of the different LV contractile parameters.

It should be noted that:

$$\left| R(t) \frac{d^2R}{dt^2} \right| \gg 2 \cdot \left(\frac{dR}{dt}\right)^2. \tag{39}$$

Therefore, the acceleration of aortic blood flow and the acceleration of the LV wall can be approximately interrelated using:

$$\frac{-4}{r^2} R^2(t) \frac{d^2R}{dt^2} \approx k \frac{dv}{dt}. \tag{40}$$

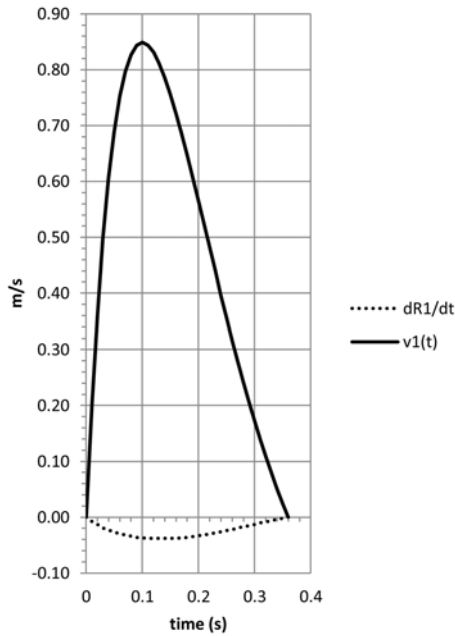


Fig. 6. Note that the velocity of blood flow within the distal thoracic aorta, $v1(t)$, peaks slightly before the maximum absolute value of the radial velocity of the LV, $dR1/dt$. Furthermore, the radial velocity of the LV has a negative value which is indicative of the associated reduction in LV size with contraction. In addition, the absolute value of $dR1/dt$ is markedly less than that of $v1(t)$. These data are from case 1 in the numerical results section.

Another clinically-relevant relationship can be shown by substituting (31) into either (35) or (26):

$$\frac{dR}{dt} = \frac{-r^2 k v(t)}{4 \left[R_{EDV}^3 - \frac{3}{4} r^2 SD(t) \right]^{\frac{2}{3}}} \quad 0 \leq t \leq FT. \tag{41}$$

Also, utilizing (40):

$$\frac{d^2 R}{dt^2} = \frac{-r^2 k a(t)}{4 \left[R_{EDV}^3 - \frac{3}{4} r^2 SD(t) \right]^{\frac{2}{3}}} \quad 0 \leq t \leq FT. \tag{42}$$

Inspection of (41) and (42) reveals that increases in both $\frac{dR}{dt}$ and $\frac{d^2 R}{dt^2}$ are associated with increases in r and/or $SD(t)$; as well as $v(t)$ and $a(t)$ respectively (Note that SV as a function of time, $SV(t)$, is directly proportional to $SD(t)$). Whereas an isolated increase in R_{EDV} is associated with decreases in both $\frac{dR}{dt}$ and $\frac{d^2 R}{dt^2}$.

This is relevant; as clinical studies have demonstrated that both velocity and acceleration of aortic blood flow correlate with LV contractility [17]. Whereas a pathologically enlarged

LV, from HF or cardiomyopathy secondarily from long-standing hypertension, will frequently exhibit reduced contractility [18].

The role of inertia, resistance, and elastance in assessing contractility

The afterload “seen” by the LV can have a substantial effect on clinically-observed contractile changes. Generally, a significant increase in afterload can cause a marked reduction in contractile indices [23]. In addition, a central nervous sympathetic response frequently occurs whereby afterload “reflexly” increases. This is observed with patients who are significantly volume-depleted [23] or in those who have HF [27]. Furthermore, mathematical modeling of afterload will assist in understanding $max\left(\frac{dP}{dt}\right)$.

Thus, a previously-described method to assess the components of afterload: inertia (L), resistance (Rs), and elastance (Ea) can be applied. This technique is based upon linear algebra and could be utilized on an instantaneous or “beat-to-beat” basis [9].

Expanding the continuity principle yields the following matrix relationship:

$$\begin{bmatrix} \dot{Q}_s(0) & Q_s(0) & SV(0) \\ \dot{Q}_s(FTp) & Q_s(FTp) & SV(FTp) \\ \dot{Q}_s(FT) & Q_s(FT) & SV(FT) \end{bmatrix}_{sphere} = A \cdot \begin{bmatrix} \dot{v}(0) & v(0) & SD(0) \\ \dot{v}(FTp) & v(FTp) & SD(FTp) \\ \dot{v}(FT) & v(FT) & SD(FT) \end{bmatrix}_{cylinder}. \tag{43}$$

The pressure vs. flow relationship, for both the LV and aorta, can then be represented using the spherical component of the model:

$$\begin{bmatrix} \dot{Q}_s(0) & Q_s(0) & SV(0) \\ \dot{Q}_s(FTp) & Q_s(FTp) & SV(FTp) \\ \dot{Q}_s(FT) & Q_s(FT) & SV(FT) \end{bmatrix} \cdot \begin{bmatrix} L \\ Rs \\ Ea \end{bmatrix} = \begin{bmatrix} P(0) \\ P(FTp) \\ P(FT) \end{bmatrix}. \tag{44}$$

Thus:

$$\begin{bmatrix} L \\ Rs \\ Ea \end{bmatrix} = \begin{bmatrix} \dot{Q}_s(0) & Q_s(0) & SV(0) \\ \dot{Q}_s(FTp) & Q_s(FTp) & SV(FTp) \\ \dot{Q}_s(FT) & Q_s(FT) & SV(FT) \end{bmatrix}^{-1} \cdot \begin{bmatrix} P(0) \\ P(FTp) \\ P(FT) \end{bmatrix}. \tag{45}$$

Where L , Rs , and Ea represent “net” inertia, resistance, and elastance respectively; within both the sphere and

cylinder.

Similarly, L , Rs , and Ea can also be determined, from the aorta, using the model’s cylindrical component:

$$\begin{bmatrix} L \\ Rs \\ Ea \end{bmatrix} = \frac{1}{A} \left\{ \begin{bmatrix} \dot{v}(0) & v(0) & SD(0) \\ \dot{v}(FTp) & v(FTp) & SD(FTp) \\ \dot{v}(FT) & v(FT) & SD(FT) \end{bmatrix}^{-1} \cdot \begin{bmatrix} P(0) \\ P(FTp) \\ P(FT) \end{bmatrix} \right\}. \tag{46}$$

In determining solutions to (45) and (46), curve-fitting techniques may be also used as an alternative to matrix inversion.

Within either component, pressure as a function of time, $P(t)$, can then be modeled:

$$P(t) = L \cdot \dot{Q}(t) + Rs \cdot Q(t) + Ea \cdot SV(t) \quad 0 \leq t \leq FT. \tag{47}$$

$$P(t) = A \cdot [L \cdot \dot{v}(t) + Rs \cdot v(t) + Ea \cdot SD(t)] \quad 0 \leq t \leq FT. \tag{48}$$

Thus, to maintain an equivalent blood pressure vs. time relationship, an LV which displays reduced contractility would mostly likely be associated with greater values of L , Rs , and Ea when compared to one with normal contractility.

Clinically, patients with HF will frequently exhibit significantly higher afterloads as compared to those with normal LV function [26]. Chronic hypertension-induced cardiomyopathy is also commonly associated with marked reductions in LV contractility [28].

A preliminary comparison, of this modelling scheme to other lumped parameter models, has demonstrated its potential usefulness and accuracy [9]. This model would also be worthwhile for practicing clinicians whose patients require comprehensive hemodynamic monitoring. Thus, as vasoactive medications and IV fluids are administered during surgery or other critical care situations, their subsequent effects on L , Rs , and Ea , could be assessed in real time. Continuous monitoring, of the interaction between volume status, afterload, and LV contractility, would be clinically valuable.

The maximum time rate change of pressure, $\max(\frac{dP}{dt})$, has also been examined at the beginning of systole, $t = 0$, as a measure of LV contractility [29]. Using either (47) or (48), $\max(\frac{dP}{dt})$ could be estimated:

$$\begin{aligned} \max(\frac{dP}{dt}) &= \max[L \cdot \ddot{Q}(0) + Rs \cdot \dot{Q}(0)] \\ &= \max[A \cdot [L \cdot \ddot{v}(0) + Rs \cdot \dot{v}(0)]] \end{aligned} \tag{49}$$

Note that acceleration and *surge*, the time rate change of acceleration, are both incorporated into (49). Clinically,

$\max(\frac{dP}{dt})$ in the proximal aorta is difficult to measure; requiring invasive catheterization. However, approximations of central aortic pressure, based upon peripheral arterial blood pressure, have been shown to be valid [30]. Nonetheless, the use of (49), using peripheral radial arterial and EDM measurements, demonstrates the clinical utility of $\max(\frac{dP}{dt})$ as a means of assessing contractility. Furthermore, simultaneous knowledge of afterload is essential in fully understanding contractility; especially within clinical settings.

In the absence of wave reflections, $\max(\frac{dP}{dt})$ could also be estimated using the water-hammer effect:

$$\max(\frac{dP}{dt}) = \max\left(\rho \cdot V_{pw} \cdot \frac{dv}{dt}\right). \tag{50}$$

Inspection of (50) reveals that $\max(\frac{dP}{dt})$ is a function of blood density, the acceleration of blood flow, and pulse wave velocity, V_{pw} . It should be noted that V_{pw} can be considered a “surrogate” for afterload; as it increases with vessel wall stiffness and decreases with increasing vessel diameter [31].

Force and kinetic energy

Assuming that the SV is an “object” which is initially accelerating within the aorta, the measurement of F, based upon MA and blood density, ρ , is subsequently defined as [23]:

$$F = \rho(SV)(MA) = M_{SV} \cdot MA. \tag{51}$$

Note that: $M_{SV} = \rho \cdot SV$.

Similarly, KE can also be determined with an EDM [23]:

$$KE = \frac{1}{2} \rho(SV)(PV)^2 = \frac{1}{2} M_{SV} \cdot (PV)^2. \tag{52}$$

KE is defined as the work done, by the LV, in *accelerating* the M_{SV} from a velocity of zero to PV [32] (The derivation of KE, using acceleration, is shown in *Appendix C*).

A preliminary examination of several patients, in different clinical situations, has demonstrated that F and KE may have greater discriminative power when compared to either PV or MA [23]. Thus, F and KE may be more sensitive to changes in LV contractility. However, both F and KE may also be less specific; as changes in either afterload and/or volume status will also influence both of these parameters as well.

Inspection of the contractile parameters demonstrates that they can be divided into those which are velocity-based as opposed to those which are acceleration-based. This categorization will later reveal a greater sensitivity, to changes in LV contractility, associated with acceleration-based parameters. Table 1 categorizes each parameter using this methodology.

Numerical examples

It is instructive to examine several hypothetical clinical scenarios using the sphere-to-cylinder model. Thus, an evaluation of the various contractile parameters can be observed. In addition, normalization of these data allows for dimensionless comparisons to be made.

Table 2 demonstrates three case scenarios utilizing different values for $\alpha\beta$ and γ . The resulting contractile parameters are subsequently documented. Fig. 7 displays these different aortic blood flow velocities as a function of time. Furthermore, the values of L , Rs , and Ea have also been determined for each of these cases and are shown in Table 3. All calculations were done using MATHCAD (PTC Corp. Needham, MA USA). Statistical analysis was accomplished utilizing EXCEL (Microsoft Corp. Redmond, WA USA).

For modeling purposes, the following assumptions were made: EDV = 140 ml, $\rho = 1060 \text{ kg/m}^3$, and FT = 0.36 seconds. A value of 1.1 cm was used for aortic radius, r . Table 2 illustrates the computational results whereas Fig. 8 is a graphical display of the sigmoid characteristic shape of each corresponding $EF(t)$.

In determining L , Rs , and Ea , a diastolic blood pressure (BP) of 65 mmHg was chosen along with an end-systolic BP of 90 mmHg. Furthermore, a BP of 120 mmHg was used at $t = FTp$ (Note that diastolic BP occurs at $t = 0$ whereas end-systolic BP occurs at $t = FT$. The BP occurring at FTp is near systole). These values were utilized for all three of the case

scenarios. The results of the subsequent afterload calculations are shown in Table 3.

Following the determination of the contractile parameters, normalization of these values, with respect to case scenario 1, was accomplished. These results are illustrated in Fig. 9.

RESULTS

Examination of Table 2 and Figs. 7, 8, and 9 demonstrates how decreases in PV and MA, for each case scenario, result in decreases in SV. Ultimately, EF and other derived contractile parameters are subsequently reduced. Furthermore, Table 2 documents the case-associated changes in both R_{ESV} and $Max\left|\frac{dR}{dt}\right|$ which have been derived using the *sphere-to-cylinder* model. Values for KE, F, and $Max\left(\frac{dP}{dt}\right)$ are also

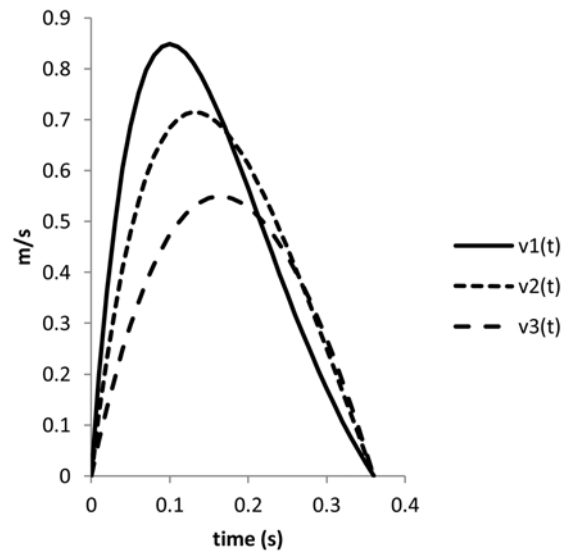


Fig. 7. Illustrated are $v1(t)$, $v2(t)$, and $v3(t)$ which represent the distal thoracic aortic blood flow velocities associated with cases 1, 2, and 3 respectively.

Table 1. LV contractile parameters can be categorized as either velocity-based or acceleration-based.

Velocity-based	Acceleration-based
PV	MA
EF	F
\overline{EF}	KE
$max\left \frac{dR}{dt}\right $	$max\left(\frac{dP}{dt}\right)$

Table 2. Three clinical case scenarios which illustrate the interrelationship of peak velocity (PV) and mean acceleration (MA), of distal thoracic aortic blood flow, to stroke volume (SV). Also illustrated are their associated derived contractility parameters. Italicized numbers, within parentheses, represent a dimensionless percentage; relative to case 1. Note that acceleration-based parameters have a statistically greater sensitivity to changes in LV contractility than those which are velocity-based ($*p = 0.00018$, $^{\#}p = 0.00015$). The equivalent spherical radius, R_{ESV} , associated with each ESV is also determined.

	Velocity-based									Acceleration-based			
	$\alpha\beta$	γ	FTp	SV	R_{ESV}	PV	EF	\overline{EF}	$max\left \frac{dR}{dt}\right $	MA	KE	F	$max\left(\frac{dP}{dt}\right)$
	(m/s^2)	(s^{-1})	(s)	(ml)	(cm)	(cm/s)	(dimensionless)	(dimensionless)	(cm/s)	(m/s^2)	(J)	(N)	(mmHg/s)
Case 1	21.75	6.154	0.1	93.2	2.24	0.849	0.666	0.404	4.31	8.49	0.036	0.84	1065
Case 2	13.05	3.2	0.132	87.2	2.33	0.715 (84)*	0.623 (94)*	0.347 (86)*	3.71 (86)*	5.42 (64)*	0.024 (67)*	0.50 (60)*	606 (57)*
Case 3	7.25	1	0.164	69.8	2.56	0.549 (65) [#]	0.499 (75) [#]	0.258 (64) [#]	2.76 (64) [#]	3.35 (39) [#]	0.011 (31) [#]	0.25 (30) [#]	262 (25) [#]
Equation(s)	19	19, 20	20	2, 5	23	19	3	18	41	12	52	51	50

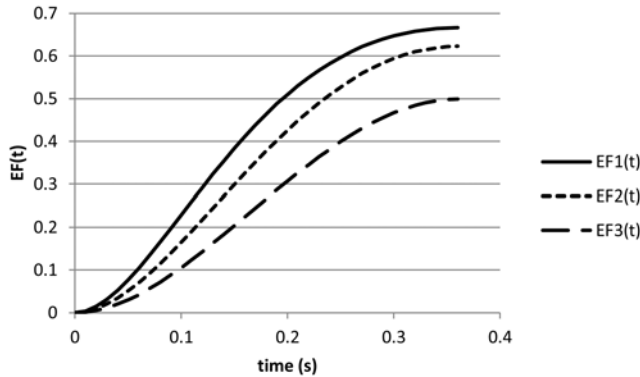


Fig. 8. Ejection fraction as a function of time, $EF(t)$, for each of the three different case scenarios. Note that at each final value: $EF(FT) = EF$.

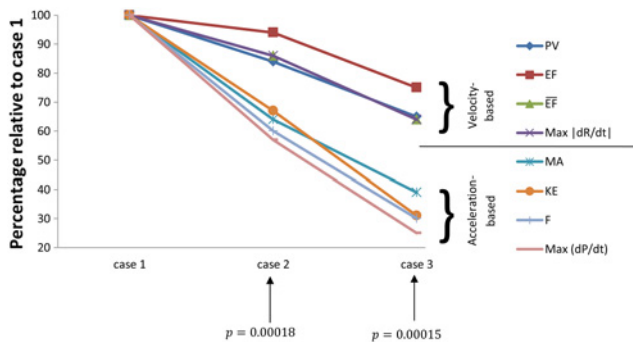


Fig. 9. An evaluation, of each parameter’s ability to numerically assess changes in LV contractility, can be accomplished by normalization to its initial value. This creates dimensionless quantities and thus provides a *relative* means of comparison. Inspection of the above graph demonstrates that acceleration-based parameters have statistically greater sensitivity to changes in LV contractility than those which are velocity-based.

presented in Table 2.

When normalized to their respective initial values associated with case 1, those contractile parameters, which are acceleration-based, have a statistically significant greater discriminative power than those which are velocity-based. This is illustrated in both Table 2 and Fig. 9.

DISCUSSION

The clinical need for continuous contractility assessment

Operative and critical care management of patients with HF represents the primary need for continuous contractility assessment. This need is not currently being met. Clinically, HF is a syndrome that, although difficult to define, is not difficult to diagnose. It can be described as the inability of the heart to meet the metabolic demands of the patient. The 2013 ACCF/AHA (American College of Cardiology

Table 3. Associated values of inertia, L ; resistance, R_s ; and elastance, E_a , for each of the three clinical scenarios.

	L (kg/m^4)	R_s ($\text{N}\cdot\text{s/m}^5$)	E_a (N/m^5)
Case 1	$1.048\cdot 10^6$	$3.589\cdot 10^7$	$1.389\cdot 10^8$
Case 2	$1.747\cdot 10^6$	$3.717\cdot 10^7$	$1.691\cdot 10^8$
Case 3	$3.144\cdot 10^6$	$3.643\cdot 10^7$	$2.584\cdot 10^8$

Foundation/American Heart Association) guidelines define HF as “a complex clinical syndrome that results from any structural or functional impairment of LV filling or ejection of blood.”

The cardinal manifestations of HF are dyspnea and fatigue, which may limit exercise tolerance, as well as fluid retention. These may subsequently lead to pulmonary and/or splanchnic congestion and/or peripheral edema [33].

In 2006, approximately 5.1 million people had HF in the United States whereas 23 million worldwide were afflicted [34]. In addition, there were more than 1 million hospitalizations with HF as the primary admitting diagnosis. Furthermore, HF accounts for 20% of all hospital admissions for persons over the age of 65 [35].

At age 40, the lifetime risk of developing HF has been found to be 20% [36]. Re-hospitalization of those patients, who had been initially discharged with a diagnosis of HF, is an important problem which is associated with a deteriorating clinical outcome, a decreasing quality of life, and an increasing cost of care.

HF has been classified into two types i.e. “diastolic HF” and “systolic HF.” However, there are more similarities than differences between these two categories [8]. Patients with diastolic HF are usually older, more likely to be women, and have a preserved EF with a normal LV cavity size; often with concentric LV hypertrophy. Patients with systolic HF are more likely to be men of all ages with a dilated LV. Patients with both types of HF have similar symptomatology including congestion, dyspnea, weakness, and a decreased exercise tolerance [8]. Since systolic as well as diastolic HF patients have impairment of both systolic and diastolic function, a more accepted classification scheme is:

- A. HF with preserved ejection fraction (HFpEF; diastolic HF)
- B. HF with reduced ejection fraction (HFrEF; systolic HF) [3].

Thus, HF may be associated with a wide spectrum of LV functional abnormalities; ranging from an LV which is normal in size with a preserved EF to severe LV dilatation with a markedly reduced EF.

In most patients with HF, abnormalities of both systolic and diastolic dysfunction coexist; irrespective of their EF [33]. It should be noted that EF is not a precise measurement

of contractility; as it is affected by changes in afterload [7]. However, it is a measurement which is easily obtained and can distinguish between HF due to systolic versus diastolic dysfunction.

The EDM may provide a more precise and continuous measurement of contractility and it may be particularly useful in evaluating those patients who are afflicted with HF with reduced EF. It is especially useful in guiding the management of patients in critical care units and during anesthesia; situations where rapid changes in volume status and afterload may occur simultaneously.

However, EDM-based measurements do not distinguish between HF which is secondary to a diffuse impairment in contractility, as is observed in dilated cardiomyopathies, versus a regional impairment of contractility (hypokinesis, akinesis, dyskinesis, LV aneurysms) which is common in coronary artery disease; where the remaining LV myocardium is hypercontractile [37]. This distinction is usually made on clinical grounds and does not affect short-term management of the patient.

This study provides the first mathematical model of LV contractility, in terms of aortic blood flow velocity and acceleration, based upon the EDM. In a straightforward manner, the contracting sphere representation of the LV, and its connection to the receiving cylindrical aorta, has allowed a comprehensive evaluation of this functional interaction. As a first approximation, the sphere-to-cylinder model has delineated that both velocity and acceleration-based contractile indices may be clinically useful.

Overall, acceleration-based parameters appear to have a greater discriminative ability than those which are velocity-based. However, F , KE , MA and $\frac{dP}{dt}$ may also be less specific to contractile changes as well. Thus, patient volume status, as well as afterload, may influence changes in acceleration-based parameters; whereas EF is fairly insensitive to changes in preload.

The derived continuous measurement, $EF(t)$, also allows LV contractility to be constantly assessed throughout the ejection phase. Furthermore, Fig. 8 illustrates the significance of $EF(t)$ during FT; the LV ejection phase. This characteristic cannot otherwise be demonstrated from a conventional LV function curve [38].

Of particular significance is that EDM-based monitoring, combined with arterial pressure measurement, also allows for clear and continuous quantification of the systemic afterload parameters which are L , R_s , and E_a [9]. With pressure held constant (For the purposes of this model, aortic blood pressure remains constant at diastole, FT_p , and end-systole for each of the three case scenarios; as described in *Methods*), the L component appears to be inversely related to the acceleration of blood flow. As shown in Table 3, changes in the L component of afterload appear to clearly differentiate

each of the three clinical scenarios.

The resistive component is related to mean pressure divided by mean flow and appears to change little with respect to changes in pulsatile flow or acceleration. Whereas the arterial elastance component is directly related to vascular stiffness and inversely proportional to arterial compliance. It reflects the significantly increased aortic stiffness associated with an increased afterload.

Note that increases in E_s have been observed, in patients with HF, where corresponding increases in systemic arterial “stiffness” have also been detected [7]. Interestingly, the L contribution to afterload is generally small when compared to the R_s component. However, its magnitude changes significantly when it is quantitatively assessed using the aforementioned matrix-inversion technique.

Limitations of the present study

The overall goal has been to present and compare LV contractile indices using EDM-based mathematical representations. This was successfully accomplished. However, there are a few limitations to the present study.

Specifically, the sphere-to-cylinder model, which describes the interaction between the LV and the aorta, appears to work well. In reality, the LV has both long and short axes which contribute differentially to contraction during systole. This characteristic could be incorporated within future studies; utilizing a hemielipsoid model.

The three case scenarios have clearly demonstrated the potential clinical utility of EDM-based contractile indices. The end-diastolic volume, EDV, fixed at 140 ml, with a varying SV, has resulted in an EF within a normal range of 0.5 to 0.67. Additional studies, which could further examine HF, would utilize an EF of 0.35 or lower. Thus, with HF subsequent dilatation of the LV chamber size arises; which would require both the EDV to be varied as well as EF. The present model is flexible enough to allow this and subsequently form an additional study; specifically related to HF.

CONCLUSIONS

There is currently no minimally-invasive clinical device which allows for continuous real-time quantitative assessment of LV contractility. The EDM, combined with peripheral arterial pressure measurements, would potentially accomplish this; simultaneously determining the influence of afterload and its related components. This is especially true for intraoperative and intensive care situations.

While EF has been the mainstay of clinical measurement of LV contractility, questions have been raised regarding its adequacy. One concerning fact is that EF does not incorporate

a “time” component. Therefore, an LV which ejects “quicker” would most likely be deemed “better” than one which ejects “slower.”

Thus, there may be a role for the clinical application of velocity and acceleration-based physical parameters. Certainly, these could be used to supplement traditional EF-based contractility assessment and not necessarily replace it.

It has been reasonably established that EF is fairly insensitive to changes in volume status. However, changes in afterload can affect EF dramatically. Similar clinical research is necessary to establish the sensitivity and specificity of both velocity-based and acceleration-based contractile parameters with respect to changes in volume and afterload. This would apply to both normal and pathologic cardiovascular states. Furthermore, the effects and side effects of pharmaceuticals on these “new” parameters would warrant additional investigation as well.

Appendix A

The velocity of distal thoracic blood flow described using Taylor’s series

The use of Taylor’s series can be helpful in numeric computational assessment of mathematical functions. Specifically, an exponential function can be described as [39] (The following definitions are utilized: $0^0 = 1$ and $0! = 1$. Note that Taylor’s series are based upon a convergent infinite summation with $n = 0, 1, 2...N$. These are usually approximated using large values for N):

$$e^{-\gamma t} = \sum_{n=0}^N \frac{(-\gamma t)^n}{n!}. \tag{1A}$$

Applying (1A) to the aortic blood flow velocity model, based upon the modified logistic Eq. (19), yields a difference of two Taylor’s series ($0 \leq t \leq FT$):

$$v(t) = (\alpha\beta) \left[\sum_{n=0}^N \frac{(-\gamma)^n (t)^{n+1}}{n!} - \frac{1}{FT} \sum_{n=0}^N \frac{(-\gamma)^n (t)^{n+2}}{n!} \right]. \tag{2A}$$

$SD_a(t)$ is subsequently generated through the use of term-by-term integration:

$$\int vtdt + C = SD_a(t) = (\alpha\beta) \left[\sum_{n=0}^N \frac{(-\gamma)^n (t)^{n+2}}{n!(n+2)} - \frac{1}{FT} \sum_{n=0}^N \frac{(-\gamma)^n (t)^{n+3}}{n!(n+3)} \right]. \tag{3A}$$

Note that $SD_a(0) = 0$ with the use of the Taylor’s series. Acceleration can also be determined:

$$\frac{d}{dt}v(t) = a(t) = (\alpha\beta) \left[\sum_{n=0}^N \frac{(n+1)(-\gamma t)^n}{n!} - \frac{1}{FT} \sum_{n=0}^N \frac{(n+2)(-\gamma)^n (t)^{n+1}}{n!} \right]. \tag{4A}$$

Appendix B

Derivation of stroke volume using the sphere-to-cylinder model

Using the continuity principle (33) applied to the *sphere-to-cylinder* model, SV can be determined:

$$\frac{-4}{r^2} \int R^2(t)dR = k \cdot \int v(t)dt + C_R. \tag{1B}$$

Expressing (1B) as a *definite* integral, the associated limits of integration are shown:

$$\frac{-4}{r^2} \int_{R_{EDV}}^{R_{ESV}} R^2(t)dR = k \cdot \int_0^{FT} v(t)dt = k \cdot SD_a. \tag{2B}$$

Note that $R(0) = R_{EDV}$ and $R(FT) = R_{ESV}$. The solution to (2B) is:

$$\frac{-4}{3r^2} [R_{ESV}^3 - R_{EDV}^3] = SD(FT) - SD(0). \tag{3B}$$

Multiplying both sides of (3B) by aortic cross sectional area, πr^2 , and recalling that $SD(0) = 0$ yields SV as defined using the *sphere-to-cylinder* model:

$$SV = \frac{4\pi}{3} [R_{EDV}^3 - R_{ESV}^3] = \pi r^2 SD(FT). \tag{4B}$$

Appendix C

Derivation of kinetic energy using acceleration.

Kinetic energy, KE, is defined as the work necessary to displace and accelerate the stroke mass ($M_{SV} = \rho \cdot SV$), M_{sv} , which is initially stationary, to its PV [32]. This is equal to the integral of the product of force, F , and differential displacement, dx . Note that F is generated by the LV; which is accelerating the M_{sv} :

$$KE(x) = \int F \cdot dx. \tag{1C}$$

Substituting $F = M_{sv} \cdot a$:

$$KE(x) = \int (M_{sv} \cdot a) dx. \tag{2C}$$

As acceleration is equal to the time-rate change of velocity or dv/dt :

$$KE(x) = \int (M_{sv} \cdot \frac{dv}{dt}) dx \tag{3C}$$

By definition, velocity is differential displacement, dx , divided by differential time, dt :

$$\frac{dx}{dt} = v \tag{4C}$$

Therefore:

$$dx = v \cdot dt \tag{5C}$$

Substituting (5C) into (3C) yields:

$$KE(v) = \int (M_{sv} \cdot \frac{dv}{dt} \cdot v) dt \tag{6C}$$

Simplifying and realizing that the M_{sv} has undergone both acceleration and displacement as it eventually reaches a PV, from an initial velocity, $v(0)$:

$$KE = \int_{v(0)}^{PV} (M_{sv} \cdot v) dv \tag{7C}$$

Thus:

$$KE = \frac{1}{2}(M_{sv}) \cdot [(PV)^2 - [v(0)]^2] = \frac{1}{2}(M_{sv}) \cdot (PV + v(0))(PV - v(0)) \tag{8C}$$

Note that the M_{sv} must undergo acceleration from $v(0)$ to PV. Recognizing that $v(0) = 0$ yields:

$$KE = \frac{1}{2}(M_{sv}) \cdot (PV)^2 \tag{9C}$$

Furthermore, $PV = MA \cdot FTp$. Substituting this expression into (9C) yields:

$$KE = \frac{1}{2}(M_{sv}) \cdot (MA \cdot FTp)^2 \tag{10C}$$

ABBREVIATIONS

Abbreviation	Term	Dimension
α	acceleration	m/s^2
β	gain	dimensionless
γ	inverse time constant	s^{-1}
ρ	density of blood	kg/m^3
$a(t)$	acceleration as a function of time	m/s^2
A	aortic cross sectional area	cm^2

BP	blood pressure	mmHg
Ea	elastance	N/m^5
EDV	end-diastolic volume	ml
ESV	end-systolic volume	ml
EF	ejection fraction	dimensionless
\overline{EF}	mean ejection fraction	dimensionless
$EF(t)$	ejection fraction as a function of time	dimensionless
F	force	N
FT	flow time	s
FTp	time to peak flow	s
HF	heart failure	
k	proportionality constant	dimensionless
KE	kinetic energy	Joules
L	inertia	kg/m^4
LV	left ventricle	
$max\left \frac{dR}{dt}\right $	maximum absolute value of the radial velocity of LV shortening	cm/s
$max\left(\frac{dP}{dt}\right)$	maximum time rate change of systolic blood pressure	mmHg/s
M_{sv}	stroke mass $M_{SV} = \rho \cdot SV$	kg
PV	peak velocity	cm/s
$Pv(t)$	velocity of right ventricular outflow	cm/s
$P(t)$	arterial blood pressure as a function of time	mmHg
$Q_c(t)$	flow into the cylindrical component of the model as a function of time	cm^3/s
$Q_s(t)$	flow from the spherical component of the model as a function of time	cm^3/s
r	aortic radius	cm
$R(t)$	radius of the spherical component of the model as a function of time	cm
R_{EDV}	radius of the spherical model associated with end-diastolic volume	cm
R_{ESV}	radius of the spherical model associated with end-systolic volume	cm
Rs	resistance	$N \cdot s/m^5$
$SDa(t)$	stroke distance associated with blood flow in the distal thoracic aorta as a function of time	cm
$SD(t)$	stroke distance as a function of time	cm

SV	stroke volume	cm
$SV(t)$	stroke volume as a function of time	cm
$v(t)$	velocity of distal aortic blood flow as a function of time	cm/s
\bar{v}	mean velocity of distal aortic blood flow	cm/s
$V(t)$	volume of blood ejected from the sphere as a function of time	cm ³
V_{pw}	pulse wave velocity	m/s

ACKNOWLEDGEMENTS

The authors would like to acknowledge Arthur Ritter, Ph.D. for his advice and assistance.

CONFLICT OF INTEREST STATEMENTS

Atlas G declares that he has no conflict of interest in relation to the work in this article. Li JK-J declares that he has no conflict of interest in relation to the work in this article. Kostis JB declares that he has no conflict of interest in relation to the work in this article. Disclosures: The authors have no financial interest in any product associated with this research.

REFERENCES

- [1] Li JK-J. The arterial circulation: physical principles and clinical applications. Totowa, NJ: Humana Press; 2000.
- [2] Robotham JL, Takata M, Berman M, Harasawa Y. Ejection fraction revisited. *Anesthesiology*. 1991; 74(1):172-83.
- [3] Davis BR, Kostis JB, Simpson LM, Black HR, Cushman WC, Einhorn PT, Farber MA, Ford CE, Levy D, Massie BM, Nawaz S. Heart failure with preserved and reduced left ventricular ejection fraction in the antihypertensive and lipid-lowering treatment to prevent heart attack trial. *Circulation*. 2008; 118(22):2259-67.
- [4] Abbas SM, Hill AG. Systematic review of the literature for the use of oesophageal Doppler monitor for fluid replacement in major abdominal surgery. *Anaesthesia*. 2008; 63(1):44-51.
- [5] DiCorte CJ, Latham P, Greulich PE, Cooley MV, Grayburn PA, Jessen ME. Esophageal Doppler monitor determinations of cardiac output and preload during cardiac operations. *Ann Thorac Surg*. 2000; 69(6):1782-6.
- [6] Nixon JV, Murray RG, Leonard PD, Mitchell JH, Blomqvist CG. Effect of large variations in preload on left ventricular performance characteristics in normal subjects. *Circulation*. 1982; 65(4):698-703.
- [7] Kerkhof PL, Li JK, Heyndrickx GR. Effective arterial elastance and arterial compliance in heart failure patients with preserved ejection fraction. *Conf Proc IEEE Eng Med Biol Soc*. 2013; 691-4.
- [8] Jessup M, Brozena S. Heart failure. *N Engl J Med*. 2003; 348(20):2007-18.
- [9] Atlas GM. Development and application of a logistic-based systolic model for hemodynamic measurements using the esophageal Doppler monitor. *Cardiovasc Eng*. 2008; 8(3):159-73.
- [10] Boulnois JL, Pechoux T. Non-invasive cardiac output monitoring by aortic blood flow measurement with the Dynemo 3000. *J Clin Monit Comput*. 2000; 16(2):127-40.
- [11] Lavandier B, Cathignol D, Muchada R, Xuan BB, Motin J. Noninvasive aortic blood flow measurement using an intraesophageal probe. *Ultrasound Med Biol*. 1985; 11(3):451-60.
- [12] Atlas GM. Can the Esophageal Doppler Monitor Be Used to Clinically Evaluate Peak Left Ventricle dP/dt? *Cardiovasc Eng*. 2002; 2(1):1-6.
- [13] Wolak A, Gransar H, Thomson LE, Friedman JD, Hachamovitch R, Gutstein A, Shaw LJ, Polk D, Wong ND, Saouaf R, Hayes SW, Rozanski A, Slomka PJ, Germano G, Berman DS. Aortic size assessment by noncontrast cardiac computed tomography: normal limits by age, gender, and body surface area. *J Am Coll Cardiol: Cardiovasc Imaging*. 2008; 1(2):200-9.
- [14] Monnet X, Robert JM, Jozwiak M, Richard C, Teboul JL. Assessment of changes in left ventricular systolic function with oesophageal Doppler. *Brit J Anaesth*. 2013; 111(5):743-9.
- [15] Fogel MA. Use of ejection fraction (or lack thereof), morbidity/mortality and heart failure drug trials: a review. *Int J Cardiol*. 2002; 84(2-3):119-32.
- [16] Isaz K, Ethevenot G, Admant P, Brembilla B, Pernot C. A new Doppler method of assessing left ventricular ejection force in chronic congestive heart failure. *Am J Cardiol*. 1989; 64(1):81-7.
- [17] Sabbah HN, Khaja F, Brymer JF, McFarland TM, Albert DE, Snyder JE, Goldstein S, Stein PD. Noninvasive evaluation of left ventricular performance based on peak aortic blood acceleration measured with a continuous-wave Doppler velocity meter. *Circulation*. 1986; 74(2):323-9.
- [18] Sabbah HN, Gheorghide M, Smith ST, Frank DM, Stein PD. Serial evaluation of left ventricular function in congestive heart failure by measurement of peak aortic blood acceleration. *Am J Cardiol*. 1988; 61(4):367-70.
- [19] Atlas G, Mort T. Placement of the esophageal Doppler ultrasound monitor probe in awake patients. *Chest*. 2001; 119(1):319.
- [20] English J, Moppett I. Assessment of a new nasally placed transoesophageal Doppler probe in awake volunteers: A-77. *Eur J Anaesth*. 2004; 21:20.
- [21] Wang D, Atlas G. Use of the esophageal Doppler monitor in prone-positioned patients. *Conf Proc NY State Soc Anesthesiol*. 2009.
- [22] Yang SY, Shim JK, Song Y, Seo SJ, Kwak YL. Validation of pulse pressure variation and corrected flow time as predictors of fluid responsiveness in patients in the prone position. *Brit J Anaesth*. 2013; 110(5):713-20.
- [23] Atlas G, Brealey D, Dhar S, Dikta G, Singer M. Additional hemodynamic measurements with an esophageal Doppler monitor: a preliminary report of compliance, force, kinetic energy, and afterload in the clinical setting. *J Clin Monitor Comp*. 2012; 26(6):473-82.
- [24] Jung B, Schneider B, Markl M, Saubier B, Geibel A, Hennig J. Measurement of left ventricular velocities: phase contrast MRI velocity mapping versus tissue-Doppler-ultrasound in healthy volunteers. *J Cardiovasc Magn Reson*. 2004; 6(4):777-83.
- [25] Kvitting JP, Ebbens T, Wigström L, Engvall J, Olin CL, Bolger AF. Flow patterns in the aortic root and the aorta studied with

- time-resolved, 3-dimensional, phase-contrast magnetic resonance imaging: implications for aortic valve-sparing surgery. *J Thorac Cardio Surg.* 2004; 127(6):1602-7.
- [26] Lind B, Nowak J, Cain P, Quintana M, Brodin LÅ. Left ventricular isovolumic velocity and duration variables calculated from colour-coded myocardial velocity images in normal individuals. *Eur J Echocardiogr.* 2004; 5(4):284-93.
- [27] Finkelstein SM, Cohn JN, Collins VR, Carlyle PF, Shelley WJ. Vascular hemodynamic impedance in congestive heart failure. *Am J Cardiol.* 1985; 55(4):423-7.
- [28] Levy D, Larson MG, Vasani RS, Kannel WB, Ho KK. The progression from hypertension to congestive heart failure. *J Am Med Assoc.* 1996; 275(20):1557-62.
- [29] Yamada H, Oki T, Tabata T, Iuchi A, Ito S. Assessment of left ventricular systolic wall motion velocity with pulsed tissue Doppler imaging: comparison with peak dp/dt of the left ventricular pressure curve. *J Am Soc Echocardiogr.* 1998; 11(5):442-9.
- [30] Tartière JM, Tabet JY, Logeart D, Tartière-Kesri L, Beauvais F, Chavelas C, Cohen Solal A. Noninvasively determined radial dp/dt is a predictor of mortality in patients with heart failure. *Am Heart J.* 2008; 155(4):758-63.
- [31] Atlas G, Li JK-J. Brachial artery differential characteristic impedance: Contributions from changes in young's modulus and diameter. *Cardiovasc Eng.* 2009; 9(1):11-7.
- [32] Benenson W, Harris JW, Stöcker H, Lutz H. *Handbook of physics.* 1st ed. New York: Springer; 2002.
- [33] Yancy CW, Jessup M, Bozkurt B, Butler J, Casey DE Jr, Drazner MH, Fonarow GC, Geraci SA, Horwich T, Januzzi JL, Johnson MR, Kasper EK, Levy WC, Masoudi FA, McBride PE, McMurray JJ, Mitchell JE, Peterson PN, Riegel B, Sam F, Stevenson LW, Tang WH, Tsai EJ, Wilkoff BL. 2013 ACCF/AHA guideline for the management of heart failure: executive summary A report of the American college of cardiology foundation/American heart association task force on practice guidelines. *Circulation.* 2013; 128(16):1810-52.
- [34] Go AS, Mozaffarian D, Roger VL, Benjamin EJ, Berry JD, Borden WB, Bravata DM, Dai S, Ford ES, Fox CS, Franco S, Fullerton HJ, Gillespie C, Hailpern SM, Heit JA, Howard VJ, Huffman MD, Kissela BM, Kittner SJ, Lackland DT, Lichtman JH, Lisabeth LD, Magid D, Marcus GM, Marelli A, Matchar DB, McGuire DK, Mohler ER, Moy CS, Mussolino ME, Nichol G, Paynter NP, Schreiner PJ, Sorlie PD, Stein J, Turan TN, Virani SS, Wong ND, Woo D, Turner MB. Heart disease and stroke statistics—2013 update: a report from the American heart association. *Circulation.* 2013; 127(1):e1-e245.
- [35] Lloyd-Jones D, Adams RJ, Brown TM, Carnethon M, Dai S, De Simone G, Ferguson TB, Ford E, Furie K, Gillespie C, Go A, Greenlund K, Haase N, Hailpern S, Ho PM, Howard V, Kissela B, Kittner S, Lackland D, Lisabeth L, Marelli A, McDermott MM, Meigs J, Mozaffarian D, Mussolino M, Nichol G, Roger VL, Rosamond W, Sacco R, Sorlie P, Stafford R, Thom T, Wasserthiel-Smoller S, Wong ND, Wylie-Rosett J. Executive summary: heart disease and stroke statistics—2010 update: a report from the American heart association. *Circulation.* 2010; 121(7):948-54.
- [36] Lloyd-Jones D, Larson MG, Leip EP, Beiser A, D'Agostino RB, Kannel WB, Murabito JM, Vasani RS, Benjamin EJ, Levy D. Lifetime risk for developing congestive heart failure. The framingham heart study. *Circulation.* 2002; 106(24):3068-72.
- [37] Grines CL, Topol EJ, Califf RM, Stack RS, George BS, Kereiakes D, Boswick JM, Kline E, O'Neill WW. Prognostic implications and predictors of enhanced regional wall motion of the noninfarct zone after thrombolysis and angioplasty therapy of acute myocardial infarction. The TAMI Study Groups. *Circulation.* 1989; 80(2):245-53.
- [38] Drzewiecki GM, Li, JK-J. (Eds.). *Analysis and assessment of cardiovascular function: with 106 figures.* New York: Springer; 1998.
- [39] Kreyszig, E. *Advanced engineering mathematics.* 10th ed. Hoboken, NJ: John Wiley & Sons; 2010.